

Optimal Estimate of Transmission Line Fault Location Considering Measurement Errors

Yuan Liao, *Senior Member, IEEE*, and Mladen Kezunovic, *Fellow, IEEE*

Abstract—Various transmission line fault location algorithms have been proposed in the past depending on the measurements available. These algorithms perform well when the measurements utilized are accurate; they may yield erroneous results when the measurements contain considerable errors. In some cases, there are redundant measurements available for fault location purposes, and it may be possible to design an optimal estimator for the fault location based on nonlinear estimation theories. This paper aims at proposing a possible method for deriving an optimal estimate of the fault location that is capable of detecting and identifying the bad measurement data, minimizing the impacts of the measurement errors and thus significantly improving the fault location accuracy. The solution is based on the distributed parameter line model and thus fully considers the effects of shunt capacitances of the line. Since field data are not available, case studies based on simulated data are presented for demonstrating the effectiveness of the new method.

Index Terms—Bad measurement detection and identification, distributed parameter line model, fault location, nonlinear estimation theory, optimal estimator.

I. INTRODUCTION

PROMPT and accurate location of the faults in a large-scale transmission system can accelerate the system restoration, reduce the outage time and improve the system reliability [1]–[4].

Great efforts have been made in the past developing various algorithms for improved fault location estimates [1]–[19]. One-terminal algorithms using local voltages and currents are proposed in [2], [3]. The accuracy of this type of algorithm is normally adversely affected by the fault resistance, and a compensation technique is proposed to alleviate this effect [3]. To improve the accuracy of estimation, the authors of [4] have designed a special one-end algorithm applicable to phase to ground faults. Methods for parallel line fault location using one-end data are reported in [5] and [6]. Reference [7] presents an approach using prefault and fault current phasors at one end of the line for estimating the fault location assuming the source impedances to be available. Fault location techniques employing measurements at two- or multiends of the line have been proposed in [8]–[15]. Unsynchronized measurements are

utilized for estimating the fault location and the synchronization angle between the measurements at the two terminals of the line [8]–[10]. A lumped line model is used in [8] and the shunt capacitance for long lines is compensated in an iterative way. Reference [9] is also based on the lumped model and the shunt capacitance of the line is neglected. The technique presented in [10] first obtains the synchronization angle by solving a quadratic equation and then derives the fault location, ignoring the distributed parameter effects while considering the shunt admittance of the line. Synchronized measurements have been utilized in [11]–[15]. Reference [11] formulates the fault location problem based on the travelling wave equations considering losses. The ABCD parameters of the line are utilized in [13] and [14] for deriving the fault location based on the lumped line model. Synchronized voltage measurements from multiends of the lines are utilized to find the fault location assuming that the source impedances are known without considering the shunt capacitance in [15]. A method based on the fault generated transients and the travelling wave theory is presented in [16]. A genetic algorithm based method that formulates the fault location problem as an optimization problem and searches the fault through the network is described in [17]. Neural network based approaches have been explored in [18] and [19].

Among these algorithms, some use voltages, some use currents, and some utilize both. Some assume source impedances are available, and some do not. Some utilize only the measurements during the fault while others also draw on the prefault measurements.

These existing algorithms perform well when the measurements utilized are accurate. In practice sometimes the measurements may contain errors due to various reasons such as the current transformer saturation, data conversion errors or communication device abnormalities [20], [21]. If the selected measurements contain large errors, the algorithms could lead to considerable errors in fault location estimate.

Therefore, it will be very desirable if a fault location approach can be designed with a capability for detecting and identifying errors in the measurements. In this way, the bad measurements would be removed and only the good measurements utilized to achieve a more accurate estimate of the fault location.

This paper proposes a method for fault location able to make the most of all the measurements available and minimize the impacts of measurement errors. The proposed solution is based on the fundamental frequency phasors, which can be calculated from recorded waveforms or directly obtained from measuring devices such as phasor measurement units. A two terminal transmission line model is utilized in illustrating the solution.

Section II presents the proposed method. The evaluation studies are reported in Section III, followed by the conclusion.

Manuscript received February 6, 2006; revised April 18, 2006. Paper no. TPWRD-00057-2006.

Y. Liao is with the Department of Electrical and Computer Engineering, University of Kentucky, Lexington, KY 40506 USA (e-mail: yliao@engr.uky.edu).

M. Kezunovic is with the Department of Electrical and Computer Engineering, Texas A&M University, College Station, TX 77843-3128 USA (e-mail: kezunov@ece.tamu.edu).

Digital Object Identifier 10.1109/TPWRD.2007.899554



Fig. 1. Transmission line considered for analysis.

II. PROPOSED OPTIMAL ESTIMATOR FOR FAULT LOCATION

Section II-A presents the overall description of the proposed method. Section II-B and II-C illustrates the method in detail. Section II-D describes the procedure for detecting and identifying possible bad measurements.

A. Overall Description of the Method

Consider the line, assumed to be a transposed line, between terminals P and Q as shown in Fig. 1, where E_G and E_H represent the Thevenin equivalent sources. The equivalent π circuit based on the distributed parameter line model is utilized to automatically and fully consider shunt capacitances and distributed parameter effects of long lines.

Generally speaking, the data available for fault location purposes may include: prefault voltage and current data, fault voltage and current data, Thevenin equivalent source voltages and impedances, and the synchronization angle between measurements at P and Q. For a balanced three phase circuit, there are normally only the positive sequence components in the prefault network. There may be positive-, negative- and zero-sequence components in the network during the fault depending on the fault type. Due to uncertainty of the values of Thevenin equivalent parameters, Thevenin source voltages and impedances are preferred not to be utilized for fault location. Then, based on the Kirchhoff voltage and current law, the following types of equations utilizing appropriate measurements can be derived [22].

- Equations linking the prefault voltages, currents and the synchronization angle based on the prefault positive sequence network.
- Equations linking the fault voltages, currents, the fault location and the synchronization angle based on the fault positive, negative or zero sequence network, whichever is appropriate depending on the fault type.
- Equations linking the superimposed voltages, currents, the fault location and the synchronization angle based on the fault positive, negative or zero sequence network, whichever is appropriate depending on the fault type.

Since the measurements and the phasor estimates may contain errors, estimation of fault location based on a single equation could be unreliable. On the other hand, a set of redundant equations may be derived with the fault location being the unknown variable. Therefore, the nonlinear estimation theory may be utilized to obtain an optimal estimate of the fault location and each of the phasors. Statistical approaches can also be adopted to detect, identify and remove any possible bad data, and thus improve the fault location accuracy and increase the robustness of the algorithm by minimizing the impacts of possible measurement errors. More accurate estimates of the fault location and phasors can further lead to more accurate calculation of the current and voltage at the fault point and the fault impedance. The proposed approach is illustrated in the following sections.

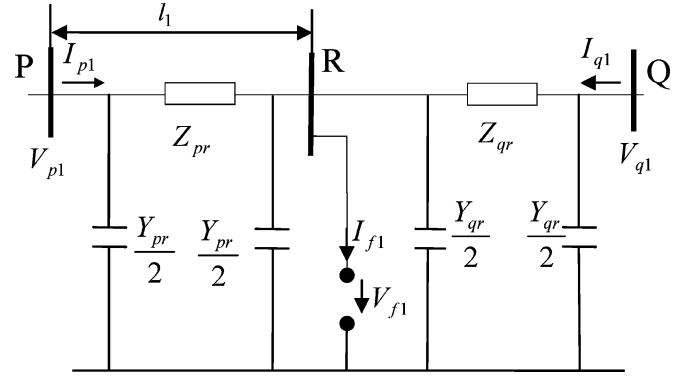


Fig. 2. Positive sequence network of the system during the fault.

B. Proposed Optimal Estimator

The following discussion assumes that synchronized voltage and current measurements at P and Q prior to and during the fault are available. Fig. 2 depicts the positive sequence network of the system during the fault. R represents the fault point.

The following notations are adopted.

V_{p1}, I_{p1}	positive sequence voltage and current during the fault at P;
V_{q1}, I_{q1}	positive sequence voltage and current during the fault at Q;
Z_{pr}, Z_{qr}	equivalent series impedance of the line segment PR and QR;
Y_{pr}, Y_{qr}	equivalent shunt admittance of the line segment PR and QR;
V_{pn}, I_{pn}	prefault positive sequence voltage and current at P;
V_{qn}, I_{qn}	prefault positive sequence voltage and current at Q;
$\Delta V_{p1}, \Delta I_{p1}$	positive sequence superimposed voltage and current at P caused by the fault;
$\Delta V_{q1}, \Delta I_{q1}$	positive sequence superimposed voltage and current at Q caused by the fault;
I_{f1}, V_{f1}	positive sequence fault currents and voltages at fault point R;
l_1	fault distance from P to R in mile or km.

Based on Fig. 2, we can derive the following equation:

$$V_{p1} - Z_{pr} \left(I_{p1} - V_{p1} \frac{Y_{pr}}{2} \right) = \left[V_{q1} - Z_{qr} \left(I_{q1} - V_{q1} \frac{Y_{qr}}{2} \right) \right] e^{j\delta} \quad (1)$$

where δ is the synchronization angle between measurements at P and Q, representing any possible synchronization error. The equivalent line parameters are calculated based on the distributed parameter line model as follows [22]:

$$Z_c = \sqrt{z_1/y_1} \quad (2)$$

$$\gamma = \sqrt{z_1 y_1} \quad (3)$$

$$Z_{pr} = Z_c \sinh(\gamma l_1) \quad (4)$$

$$Z_{qr} = Z_c \sinh[\gamma(l - l_1)] \quad (5)$$

$$Y_{pr} = \frac{2}{Z_c} \tanh\left(\frac{\gamma l_1}{2}\right) \quad (6)$$

$$Y_{qr} = \frac{2}{Z_c} \tanh\left[\frac{\gamma(l - l_1)}{2}\right] \quad (7)$$

where

- Z_c characteristic impedance of the line;
 γ propagation constant of the line;
 l length of the line in mile or km;
 z_1, y_1 positive sequence series impedance and shunt admittance of the line per mile or km, respectively.

Substituting (4)–(7) into (1) leads to

$$V_{p1} - Z_c \sinh(\gamma l_1) \left[I_{p1} - V_{p1} \frac{1}{Z_c} \tanh\left(\frac{\gamma l_1}{2}\right) \right] - V_{q1} e^{j\delta} + Z_c \sinh[\gamma(l-l_1)] \left[I_{q1} - V_{q1} \frac{1}{Z_c} \tanh\frac{\gamma(l-l_1)}{2} \right] e^{j\delta} = 0. \quad (8)$$

If the positive sequence superimposed components are utilized, it will follow that:

$$\begin{aligned} & \Delta V_{p1} - Z_c \sinh(\gamma l_1) \left[\Delta I_{p1} - \Delta V_{p1} \frac{1}{Z_c} \tanh\left(\frac{\gamma l_1}{2}\right) \right] \\ & - \Delta V_{q1} e^{j\delta} + Z_c \sinh[\gamma(l-l_1)] \\ & \times \left[\Delta I_{q1} - \Delta V_{q1} \frac{1}{Z_c} \tanh\frac{\gamma(l-l_1)}{2} \right] e^{j\delta} = 0. \quad (9) \end{aligned}$$

Utilizing the pre-fault positive sequence components, we further derive:

$$V_{pn} - Z_c \sinh(\gamma l) \left[I_{pn} - V_{pn} \tanh(\gamma l/2)/Z_c \right] - V_{qn} e^{j\delta} = 0. \quad (10)$$

It is noted that more equations in addition to (8)–(10) may be derived depending on available data. The intention here is not to derive all the possible equations, but to illustrate how to obtain an optimal estimate of the fault location based on available measurements. The following discussion will be based on (8)–(10), and will apply equally when more measurements or equations are included.

The phasors in (8)–(10) and synchronization angle are considered as known measurements. Define

$$M = [V_{pn}, I_{pn}, V_{qn}, I_{qn}, V_{p1}, I_{p1}, V_{q1}, I_{q1}, \delta]. \quad (11)$$

The superimposed components can be computed as the difference between the fault phasors and the pre-fault phasors. δ will be assigned a value of zero since synchronized measurements are utilized. Modeling δ in the system equations could detect potential synchronization errors due to synchronizing device failures, as shown in Section III. $M_i, i = 1, \dots, 9$, is utilized to represent the i^{th} element of M .

We define the measurement functions for each of the measurements as

$$Y_i(X) = x_{2i-1} e^{jx_{2i}}, \quad i = 1, \dots, 8 \quad (12)$$

$$Y_9(X) = x_{17} \quad (13)$$

where X denotes the unknown variable vector, defined as

$$X = [x_1, x_2, x_3, \dots, x_{18}]^T \quad (14)$$

where T represents vector or matrix transpose operator. x_{18} is the fault location, i.e., $l_1 = x_{18}$.

By using the defined state variables, (8)–(10) can be written as $f_1(X) = 0$, $f_2(X) = 0$ and $f_3(X) = 0$, respectively. For example, (8) becomes

$$\begin{aligned} f_1(X) &= x_9 e^{jx_{10}} - Z_c \sinh(\gamma x_{18}) \\ & \times \left[x_{11} e^{jx_{12}} - \frac{1}{Z_c} x_9 e^{jx_{10}} \tanh\left(\frac{\gamma x_{18}}{2}\right) \right] \\ & - x_{13} e^{jx_{14}} e^{jx_{17}} + Z_c \sinh[\gamma(l-x_{18})] \\ & \times \left[x_{15} e^{jx_{16}} - \frac{1}{Z_c} x_{13} e^{jx_{14}} \tanh\frac{\gamma(l-x_{18})}{2} \right] e^{jx_{17}} \\ & = 0 \quad (15) \end{aligned}$$

$f_2(X)$ and $f_3(X)$ can be derived similarly and are not shown here.

Define S as the measurement vector

$$S_i = 0, \quad i = 1, \dots, 6 \quad (16)$$

$$S_{2i+5} = \text{Re}(M_i), \quad i = 1, \dots, 8 \quad (17)$$

$$S_{2i+6} = \text{Im}(M_i), \quad i = 1, \dots, 8 \quad (18)$$

$$S_{23} = M_9 \quad (19)$$

where $\text{Re}(\cdot)$ and $\text{Im}(\cdot)$ yield the real and imaginary part of the input argument, respectively.

Define $F(X)$ as a function vector composed of the following functions:

$$F_{2i-1}(X) = \text{Re}(f_i(X)), \quad i = 1, \dots, 3 \quad (20)$$

$$F_{2i}(X) = \text{Im}(f_i(X)), \quad i = 1, \dots, 3 \quad (21)$$

$$F_{2i+5}(X) = \text{Re}(x_{2i-1} e^{jx_{2i}}), \quad i = 1, \dots, 8 \quad (22)$$

$$F_{2i+6}(X) = \text{Im}(x_{2i-1} e^{jx_{2i}}), \quad i = 1, \dots, 8 \quad (23)$$

$$F_{23}(X) = x_{17}. \quad (24)$$

The measurement vector and the function vector are related by

$$S = F(X) + \mu \quad (25)$$

where μ is characterized by

$$R = E(\mu\mu^T) = \text{diag}(\sigma_1^2, \dots, \sigma_N^2). \quad (26)$$

$E(\cdot)$ represents the expected value and $\text{diag}(\cdot)$ symbols a diagonal matrix with diagonal elements reflecting the error variances of the measurement meters. N is the total number of measurements. Elements of R can be specified according to the accuracy of the meters, a smaller value of which indicates a more accurate measurement. If R is not known, the measurements can be assumed as equally accurate.

The optimal estimate of X is obtained by minimizing the cost function defined as

$$J = [S - F(X)]^T R^{-1} [S - F(X)]. \quad (27)$$

The solution of (27) can be derived following an iterative procedure [23]. In k^{th} iteration, the unknowns are updated using the following equations:

$$X_{k+1} = X_k + \Delta X \quad (28)$$

$$\Delta X = (H^T R^{-1} H)^{-1} \{H^T R^{-1} [S - F(X_k)]\} \quad (29)$$

$$H = \frac{\partial F(X_k)}{\partial X} \quad (30)$$

where

X_k, X_{k+1} variable vector before and after k^{th} iteration;
 k iteration number starting from 1;
 ΔX variable update.

H is composed of the derivatives of the functions with respect to the unknown variables, derivation of which is presented in Section II-C.

The iterative process can be terminated when the variable update is less than the specified tolerance. Assuming per unit value is used, then the initial value for X can be set as: one for the phasor magnitude, zero for the phasor angle, zero for the synchronization angle, and $l/2$ for the fault location.

After X is obtained, (12), (13) can be used to compute the estimated values of the measurements.

C. Derivation of the Derivatives of the Functions With Respect to Unknown Variables

The derivatives of functions $f_1(X)$, $f_2(X)$, $f_3(X)$ and $Y_i(X)$, $i = 1, \dots, 9$ with respect to the unknown variables can be readily derived. For example, we have

$$\frac{\partial f_1(X)}{\partial x_i} = 0, \quad i = 1, \dots, 8 \quad (31)$$

$$\frac{\partial f_1(X)}{\partial x_9} = e^{jx_{10}} + \sinh(\gamma x_{18}) \tanh\left(\frac{\gamma x_{18}}{2}\right) e^{jx_{10}}. \quad (32)$$

Then, the derivatives of each function in vector $F(X)$ with respect to each variable in vector X can be calculated. For example, we have

$$\frac{\partial F_1(X)}{\partial x_1} = \text{Re}\left(\frac{\partial f_1(X)}{\partial x_1}\right). \quad (33)$$

D. Detection and Identification of Bad Measurements

To detect the presence of bad measurement data, the following classical method can be utilized [22], [23]:

- Step 1) Calculate the expected value of the cost function, E_J , as the number of measurements minus the number of variables.
 Step 2) Calculate the actual value of the cost function as

$$C_J = \sum_{i=1}^L \frac{(S_i - \bar{S}_i)^2}{\sigma_i^2} \quad (34)$$

where \bar{S}_i is the estimated measurement value obtained from (12), (13) and (28)–(30), and L is the total number of measurements.

- Step 3) If $C_J > AE_J$, then the presence of bad data is suspected; otherwise, no bad data exists. A is a preselected constant such as 3.0.

If bad data exists, the largest normalized error based method can be followed to identify the bad data. First, the normalized error is calculated as

$$SE_i = \frac{S_i - \bar{S}_i}{\sqrt{\Omega_{ii}}}, \quad i = 1, \dots, N \quad (35)$$

where Ω_{ii} is the diagonal element of the matrix

$$\Omega = R - H(H^T R^{-1} H)^{-1} H^T. \quad (36)$$

Then, the measurement corresponding to the largest normalized error will be identified as the bad data. More sophisticated approaches could be utilized for bad data identification [23].

III. CASE STUDIES

This section presents the case studies demonstrating the procedure and the effectiveness of the proposed solution for detecting and identifying possible bad measurements and thus deriving a more accurate estimate of the fault location.

The Electromagnetic Transients Program (EMTP) has been employed to simulate fault cases for analyzing the proposed algorithm [24]. A 500 kV, 200 mile transmission line was modeled, which is taken from page 1622 of [15]. The transmission line was modeled using the distributed parameter line model. Different faults with various fault resistances have been simulated at different locations on the transmission line. The algorithm has been implemented in Matlab. Representative results are reported in this section.

The per unit system is utilized in the following discussions, with a base voltage of 500 kV, base voltampere of 100 MVA, and base current of 115.47 A.

In all the cases, the following starting values are utilized: one for voltage and current magnitude, zero for voltage and current angle, zero for the synchronization angle, and $l/2$ for the fault location. The estimator achieves the optimal estimate of the fault location quickly, around ten iterations for all the cases.

A. Cases Without Bad Measurements

This subsection studies the behavior of the algorithm when there are no bad measurements.

Choosing different values for the error variance matrix R will result in different estimates. In the following discussions, we will first assume that all the measurements are equally accurate, and then we will assume that the synchronization accuracy is more accurate than other measurements.

Assuming that all the measurements have the same error variance value of $1E-4$, the optimal estimates of the fault location and phasors for a phase A to ground fault with a fault resistance of 10 ohm and a fault location of 10 miles (0.05 p.u.) from terminal P are shown in Table I. The measured values and the optimal estimates are shown in the 2nd and 3rd column, respectively. The fault location in the 2nd column indicates the actual fault location.

The expected value of the cost function E_J is computed as equal to 5.0, and the actual value of the cost function C_J is

TABLE I
OPTIMAL ESTIMATES OF FAULT LOCATION AND PHASORS
WITHOUT BAD MEASUREMENTS ($\sigma_{\delta}^2 = 1E - 4$)

Quantity	Measured values	Optimal estimates
V_{pn} (p.u.)	0.9883 + j0.25138	0.9885 + j0.25141
I_{pn} (p.u.)	2.982 + j3.8553	2.982 + j3.8553
V_{qn} (p.u.)	1.0168 + j0.055805	1.0166 + j0.055745
I_{qn} (p.u.)	-3.5155 - j0.11666	-3.5155 - j0.11667
V_{p1} (p.u.)	0.71849 + j0.12928	0.71838 + j0.12954
I_{p1} (p.u.)	13.8935 - j6.8264	13.8935 - j6.8264
V_{q1} (p.u.)	0.92743 + j0.012643	0.92752 + j0.012401
I_{q1} (p.u.)	0.12141 - j3.762	0.12142 - j3.762
δ (degrees)	0	-0.012786
Fault location (p.u.)	0.05	0.04973

TABLE II
OPTIMAL ESTIMATES OF FAULT LOCATION AND PHASORS
WITHOUT BAD MEASUREMENTS ($\sigma_{\delta}^2 = 1E - 6$)

Quantity	Measured values	Optimal estimates
V_{pn} (p.u.)	0.9883 + j0.25138	0.9885 + j0.25148
I_{pn} (p.u.)	2.982 + j3.8553	2.982 + j3.8553
V_{qn} (p.u.)	1.0168 + j0.055805	1.0166 + j0.05567
I_{qn} (p.u.)	-3.5155 - j0.11666	-3.5155 - j0.11667
V_{p1} (p.u.)	0.71849 + j0.12928	0.71837 + j0.12956
I_{p1} (p.u.)	13.8935 - j6.8264	13.8935 - j6.8264
V_{q1} (p.u.)	0.92743 + j0.012643	0.92753 + j0.012381
I_{q1} (p.u.)	0.12141 - j3.762	0.12142 - j3.762
δ (degrees)	0	-0.00018019
Fault location (p.u.)	0.05	0.049679

calculated as $J = 0.0037198$. Since C_J is much less than E_J , it is concluded based on Section II-D that no bad data exists.

Assuming that the error variance of the synchronization angle is $1E-6$ and variances of the other measurements are $1E-4$, the estimates for the same fault case are shown in Table II.

The actual value of the cost function C_J is 0.0041404, which clearly indicates no presence of bad data.

It can be seen that very accurate estimates have been achieved by the proposed method. Similarly accurate results have been obtained for other types of faults with diverse fault locations.

B. Cases With Bad Synchronization

Although synchronization based on global positioning system is normally highly precise, synchronization errors still may arise due to various reasons such as improper hardware wiring, unavailability of the global positioning system (GPS) time reference and communication problems. This subsection illustrates how such errors may be pinpointed by the proposed method.

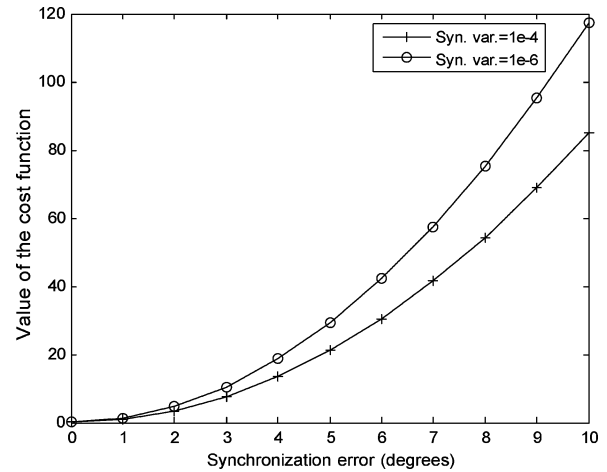


Fig. 3. Cost function versus the synchronization errors.

TABLE III
OPTIMAL ESTIMATES OF FAULT LOCATION AND
PHASORS WITH BAD SYNCHRONIZATION

Quantity	Measured values	Optimal estimates
V_{pn} (p.u.)	0.9883 + j0.25138	0.98694 + j0.22463
I_{pn} (p.u.)	2.982 + j3.8553	2.9835 + j3.856
V_{qn} (p.u.)	1.0178 - j0.033026	1.0176 - j0.0032194
I_{qn} (p.u.)	-3.5123 + j0.19018	-3.5122 + j0.19032
V_{p1} (p.u.)	0.71849 + j0.12928	0.72176 + j0.12128
I_{p1} (p.u.)	13.8935 - j6.8264	13.8935 - j6.8264
V_{q1} (p.u.)	0.925 - j0.068236	0.92222 - j0.060718
I_{q1} (p.u.)	-0.20693 - j3.7582	-0.20721 - j3.7585
δ (degrees)	0	0.020372
Fault location (p.u.)	0.05	0.070445

We first simulate a fault with specified fault conditions. Next a synchronization error is applied to the measurements at terminal Q to simulate the synchronization error. Then the estimator is applied to obtain the results and compute the value of the cost function C_J . As an example, Fig. 3 depicts the calculated value of the cost function versus the synchronization errors, for a phase A to ground fault with a fault resistance of 10 ohm and a fault location of 10 miles. One curve is obtained by using a value of $1E-6$ for synchronization variance, and the other curve using $1E-4$. Variances for other measurements are set to $1E-4$. It can be seen that the cost function becomes considerably larger when the synchronization error reaches 5° , which can be utilized to detect the presence of bad measurement data. As expected, Fig. 3 also shows that a smaller variance value of the synchronization angle makes the estimator more sensitive to synchronization errors. A more detailed analysis will be shown.

Table III lists the optimal estimates when the synchronization has an error of 5 degrees using a value of $1E-6$ for synchronization variance.

The expected value of the cost function E_J is 5.0, and the actual value of the cost function C_J is computed as 29.2704.

TABLE IV
OPTIMAL ESTIMATES OF FAULT LOCATION AND PHASORS
AFTER SYNCHRONIZATION ANGLE DATA IS REMOVED

Quantity	Measured values	Optimal estimates
V_{pn} (p.u.)	0.9883 + j0.25138	0.9885 + j0.25125
I_{pn} (p.u.)	2.982 + j3.8553	2.982 + j3.8553
V_{qn} (p.u.)	1.0178 - j0.033026	1.0176 - j0.032884
I_{qn} (p.u.)	-3.5123 + j0.19018	-3.5123 + j0.19018
V_{p1} (p.u.)	0.71849 + j0.12928	0.7184 + j0.12949
I_{p1} (p.u.)	13.8935 - j6.8264	13.8935 - j6.8264
V_{q1} (p.u.)	0.925 - j0.068236	0.92506 - j0.068435
I_{q1} (p.u.)	-0.20693 - j3.7582	-0.20692 - j3.7582
δ (degrees)	N/A	4.9564
Fault location (p.u.)	0.05	0.049855

Since C_J is noticeably greater than E_J , the presence of bad data is suspected, based on Section II-D.

To identify the possibly bad data, the normalized errors are calculated and the largest normalized error is 4.8952, which corresponds to δ . Therefore, δ is identified as the bad data. After removing δ from the measurement set, a new optimal estimate can be obtained as shown in Table IV, which indicates that a more accurate estimate of the fault location has been reached. In this case, E_J is 4.0, and the actual value of the cost function C_J is 0.0026013. Since C_J is much less than E_J , all the data are considered fairly accurate, and the estimates are regarded as acceptable.

If there is a synchronization error of 10° , the fault location estimate would be 0.092494. An improved value of 0.049855 can be achieved after the synchronization error is detected and removed.

Therefore, the optimal estimator is able to successfully detect and identify the possible synchronization errors, and obtain a more accurate fault location estimate by utilizing only the correct measurements.

C. Cases With Bad Voltage or Current Measurements

Large errors in voltage or current measurements can lead to considerable inaccuracy in fault location estimate. This subsection illustrates how such bad measurements can be detected by the optimal estimator. A value of $1E-6$ for synchronization variance and $1E-4$ for other measurements are utilized.

Suppose that there is an error of 20° in the phase angle of the prefault current measurements at terminal P, then the optimal estimates will be as shown in Table V, for a phase A to ground fault with a fault resistance of 10 ohm and a fault location of 160 miles (0.8 p.u.).

The actual value of the cost function C_J is calculated as 24.707, which is much larger than the expected value of 5.0. Therefore, presence of bad measurements is suspected and the prefault current measurement at P is identified as bad data based on the approach presented in Section II-D.

After the bad measurement is removed, a new set of optimal estimates are calculated as shown in Table VI. In this case, E_J

TABLE V
OPTIMAL ESTIMATES OF FAULT LOCATION AND PHASORS WITH BAD CURRENT MEASUREMENT

Quantity	Measured values	Optimal estimates
V_{pn} (p.u.)	0.98835 + j0.25142	0.96712 + j0.2346
I_{pn} (p.u.)	1.4806 + j4.6434	1.4819 + j4.6427
V_{qn} (p.u.)	1.0168 + j0.055844	1.0393 + j0.075062
I_{qn} (p.u.)	-3.517 - j0.11855	-3.517 - j0.11856
V_{p1} (p.u.)	0.89675 + j0.23242	0.89638 + j0.23436
I_{p1} (p.u.)	5.6142 - j0.17955	5.6141 - j0.1796
V_{q1} (p.u.)	0.83646 + j0.014976	0.83689 + j0.012943
I_{q1} (p.u.)	1.5383 - j8.258	1.5384 - j8.258
δ (degrees)	0	0.0096106
Fault location (p.u.)	0.8	0.78503

TABLE VI
OPTIMAL ESTIMATES OF FAULT LOCATION AND PHASORS WITH BAD CURRENT MEASUREMENT BEING REMOVED

Quantity	Measured values	Optimal estimates
V_{pn} (p.u.)	0.98835 + j0.25142	0.98835 + j0.25142
I_{pn} (p.u.)	N/A	2.9691 + j3.8596
V_{qn} (p.u.)	1.0168 + j0.055844	1.0168 + j0.055842
I_{qn} (p.u.)	-3.517 - j0.11855	-3.517 - j0.11855
V_{p1} (p.u.)	0.89675 + j0.23242	0.89675 + j0.23239
I_{p1} (p.u.)	5.6142 - j0.17955	5.6142 - j0.17955
V_{q1} (p.u.)	0.83646 + j0.014976	0.83645 + j0.014999
I_{q1} (p.u.)	1.5383 - j8.258	1.5383 - j8.258
δ (degrees)	0	8.443E-6
Fault location (p.u.)	0.8	0.79946

equals to 3.0, and the actual value of the cost function C_J is $1.3729E-5$. Since C_J is much less than E_J , all of the data are considered fairly accurate and the estimates are regarded as satisfactory. Comparison with Table V manifests that the fault location accuracy is considerably enhanced.

Similarly, bad voltage measurements may also be successfully detected and identified.

IV. CONCLUSION

When redundant measurements are available, this paper demonstrates that it may be feasible to design an approach for detecting, identifying and removing the possible bad measurements and thus improving the fault location estimation accuracy. More accurate estimates of the measurements such as the voltages and currents can also be achieved based on the optimal estimator, which can benefit a more precise fault analysis. When synchronized measurements are utilized, possible synchronizing errors can also be detected, thus enhancing the fault location accuracy. The developed algorithm is based on distributed parameter line model and thus fully considers the effects of shunt capacitance and distributed parameter effects

of long lines. In addition, the method is independent of source impedances. Quite encouraging results have been obtained by simulation studies.

REFERENCES

- [1] M. Kezunovic and B. Perunicic, "Fault location," in *Wiley Encyclopedia of Electrical and Electronics Terminology*. New York: Wiley, 1999, vol. 7, pp. 276–285.
- [2] K. Takagi, Y. Yomakoshi, M. Yamaura, R. Kondow, and T. Matsushima, "Development of a new type fault locator using the one-terminal voltage and current data," *IEEE Trans. Power App. Syst.*, vol. PAS-101, no. 8, pp. 2892–2898, Aug. 1982.
- [3] L. Eriksson, M. M. Saha, and G. D. Rockefeller, "An accurate fault locator with compensation for apparent reactance in the fault resistance resulting from remote-end infeed," *IEEE Trans. Power App. Syst.*, vol. PAS-104, no. 2, pp. 424–436, Feb. 1985.
- [4] Q. Zhang, Y. Zhang, W. Song, and D. Fang, "Transmission line fault location for single-phase-to-earth fault on non-direct-ground neutral system," *IEEE Trans. Power Del.*, vol. 13, no. 4, pp. 1086–1092, Oct. 1998.
- [5] Y. Liao and S. Elangovan, "Digital distance relaying algorithm for first-zone protection for parallel transmission lines," *Proc. Inst. Elect. Eng. C, Gen., Transm. Distrib.*, vol. 145, no. 5, pp. 531–536, Sep. 1998.
- [6] J. Izykowski, E. Rosolowski, and M. M. Saha, "Locating faults in parallel transmission lines under availability of complete measurements at one end," *Proc. Inst. Elect. Eng. C, Gen., Transm. Distrib.*, vol. 151, no. 2, pp. 268–273, Mar. 2, 2004.
- [7] M. Djuric, Z. Radojevic, and V. Terzija, "Distance protection and fault location utilizing only phase current phasors," *IEEE Trans. Power Del.*, vol. 13, no. 4, pp. 1020–1026, Oct. 1998.
- [8] Novosel, D. G. Hart, E. Udren, and J. Garitty, "Unsynchronized two-terminal fault location estimation," *IEEE Trans. Power Del.*, vol. 11, no. 1, pp. 130–138, Jan. 1996.
- [9] A. A. Girgis, D. G. Hart, and W. L. Peterson, "A new fault location technique for two-and three-terminal lines," *IEEE Trans. Power Del.*, vol. 7, no. 1, pp. 98–107, Jan. 1992.
- [10] M. Sachdev and R. Agarwal, "A technique for estimating transmission line fault locations from digital impedance relay measurements," *IEEE Trans. Power Del.*, vol. 13, no. 1, pp. 121–129, Jan. 1998.
- [11] A. Gopalakrishnan, M. Kezunovic, S. M. McKenna, and D. M. Hamai, "Fault location using distributed parameter transmission line model," *IEEE Trans. Power Del.*, vol. 15, no. 4, pp. 1169–1174, Oct. 2000.
- [12] Y. H. Lin, C. W. Liu, and C. S. Chen, "A new PMU-based fault detection/location technique for transmission lines with consideration of arcing fault discrimination—Part I: Theory and algorithms," *IEEE Trans. Power Del.*, vol. 19, no. 4, pp. 1587–1593, Oct. 2004.
- [13] D. J. Lawrence, L. Cabeza, and L. Hochberg, "Development of an advanced transmission line fault location system, Part II-Algorithm development and simulation," *IEEE Trans. Power Del.*, vol. 7, no. 4, pp. 1972–1983, Oct. 1992.
- [14] D. J. Lawrence, L. Cabeza, and L. Hochberg, "Development of an advanced transmission line fault location system, Part I-Input transducer analysis and requirements," *IEEE Trans. Power Del.*, vol. 7, no. 4, pp. 1963–1971, Oct. 1992.
- [15] S. M. Brahma, "Fault location on a transmission line using synchronized voltage measurements," *IEEE Trans. Power Del.*, vol. 19, no. 4, pp. 1619–1622, Oct. 2004.
- [16] F. H. Magnago and A. Abur, "Accurate fault location using wavelets," *IEEE Trans. Power Del.*, vol. 13, no. 4, pp. 1475–1480, Dec. 1998.
- [17] S. Luo, M. Kezunovic, and D. R. Sevcik, "Locating faults in the transmission network using sparse field measurements, simulation data and genetic algorithms," *Elect. Power Syst. Res.*, vol. 71, no. 2, pp. 169–177, Oct. 2004.
- [18] J. Gracia, A. J. Mazon, and I. Zamora, "Best ANN structures for fault location in single-and double-circuit transmission lines," *IEEE Trans. Power Del.*, vol. 20, no. 4, pp. 2389–2395, Oct. 2005.
- [19] R. N. Mahanty and P. B. D. Gupta, "Application of RBF neural network to fault classification and location in transmission lines," *Proc. Inst. Elect. Eng., Gen., Transm. Distrib.*, vol. 151, no. 2, pp. 201–212, Mar. 2004.
- [20] S. E. Zocholl and D. W. Smaha, "Current transformer concepts," in *Proc. 19th Annual Western Protective Relay Conf.*, Spokane, WA, Oct. 20–22, 1992.
- [21] J. R. Linders, C. W. Barnett, and J. W. Chadwick *et al.*, "Relay performance considerations with low-ratio CTs and high-fault currents," *IEEE Trans. Ind. Appl.*, vol. 31, no. 2, pp. 392–404, Mar./Apr. 1995.
- [22] J. Grainger and W. Stevenson, *Power System Analysis*. New York: McGraw-Hill, 1994.
- [23] A. Abur and A. G. Exposito, *Power System State Estimation—Theory and Implementation*. New York: Marcel Dekker, 2004.
- [24] Leuven EMTP Centre, *Alternative Transient Program, User Manual and Rule Book*. Leuven, Belgium, 1987.



Yuan Liao (S'98–M'00–SM'05) is an Assistant Professor with the Department of Electrical and Computer Engineering at the University of Kentucky, Lexington. He was an R&D Consulting Engineer and then Principal R&D Consulting Engineer with the ABB Corporate Research Center, Raleigh, NC. His research interests include protection, power market modeling and simulation, large-scale resource scheduling optimization, and EMS/SCADA design.



Mladen Kezunovic (S'77–M'80–SM'85–F'99) received the Dipl.Ing. degree in electrical engineering from the University of Sarajevo, Sarajevo, Yugoslavia, in 1974, and the M.S. and Ph.D. degrees in electrical engineering from the University of Kansas, Lawrence, in 1977 and 1980, respectively.

He was with Westinghouse Electric Corporation, Pittsburgh, PA, and the Energoinvest Company, Sarajevo. He was a Visiting Associate Professor at Washington State University, Pullman, in 1986–1987. He has been with Texas A&M University, College Station, since 1987 where he is the Eugene E. Webb Professor and Director of the Electric Power and Power Electronics Institute. His main research interests are digital simulators and simulation methods for equipment evaluation and testing as well as application of intelligent methods to control, protection and power quality monitoring.

Dr. Kezunovic is a registered professional engineer in Texas.